

MEASUREMENT OF DEFORMABILITY OF A SINGLE RED BLOOD CELL IN MICRO-CHANNELS WITH HIGH SHEAR FLOWS USING AN I-V METHOD

Yoichi KATSUMOTO*, Tatsuki DOI*, Kazuya TATSUMI* and Kazuyoshi NAKABE*

* Kyoto University, Kyoto 606-8501, Japan
E-mail : yoichi.katsumoto@fy7.ecs.kyoto-u.ac.jp

Keywords : Micro-channel, Red Blood Cell, Deformability, Micro Electric Resistance Sensor.

ABSTRACT

Deformability of a single red blood cell (RBC) flowing in a micro-channel is measured by analyzing the electric resistance detected between the membrane-type counter-electrodes of micro sensors mounted onto the channel bottom wall, where relatively large deformation of RBC is expected due to the high shear flow layers. In the first half of this work, the electric field and resistance between the electrodes under the conditions of with and without RBC were evaluated by numerical simulation to design the channel geometry and sensor arrangement. In the later part, the experiment was made in which the deformability of RBC was measured by analyzing the time series of the electric resistance obtained by the sensors using an I-V method with a frequency of 10kHz.

1. INTRODUCTION

Micro-channels are one of the useful tools to produce high shear flows and to deform RBCs. In combination with microscopic image acquisition, the RBC deformation can be visualized directly (Korin, 2007). This kind of image-based analyzing systems, however, has a disadvantage in practical use considering their throughput and compactness. On the contrary, electrically analyzing systems, such as a coulter counter for cell counting (Tang, 2005) and a dielectric spectroscopy for physical quantification of individual cells (Gawad, 2004), can monitor RBCs' behaviors with a fast succession of quantitative signals.

In the present method, the RBC deformability is evaluated from the electric resistances of RBCs passing between the counter-electrodes-type membrane sensors attached to the bottom wall of a micro-channel (see Fig. 1). High shear rate flows are applied to the RBC where the RBC changes its shape into ellipsoidal body, depending on its elastic modulus. The pattern of the resistance signal is believed to be unique to the shape of the RBC, and, therefore, the pattern is analyzed to represent the deformability of each RBC.

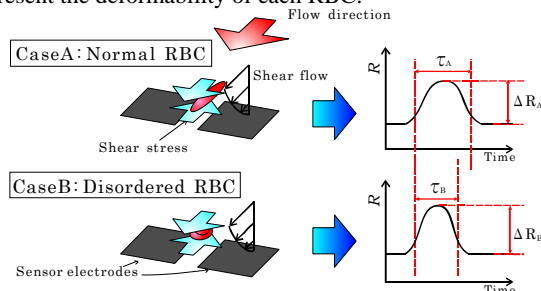


Fig. 1 Concept of the measurement for the RBC deformability.

2. SIMULATION

Three-dimensional FEM simulation was conducted for the 3D harmonic electric field under the conditions of with/without RBC using ANSYS (ANSYS Inc.). RBC solution is a heterogeneous system consisting of solvent and cytoplasm of micro-scale and cell membrane of nano-scale. In order to avoid the difficulties of handling such a discrepancy of the scales in the computation, RBC was treated as a spherical or ellipsoidal solid having frequency-dependent uniform complex permittivity, which was analytically derived from Maxwell-Wagner equation. Under the above assumptions, the frequency dependent impedance between the electrodes was calculated with high accuracy. The numerical conditions are tabulated in Table 1 and also Fig. 2.

Figure 2 shows how the deformation index, DI , affects the relation between the resistance variation, ΔR , and the streamwise position of the RBC center, x_{RBC} . DI is defined as $(a-b)/(a+b)$, where a and b are the major and minor axes of RBC, respectively. The case without the guard electrodes, which was placed to increase the sensor sensitivity, is also plotted in the figure for comparison. ΔR takes a maximum peak at $x_{RBC} = 0$ and decreases as x_{RBC} increases. The maximum value and the width of the ΔR distribution increase as DI increases. This is ascribable to the increase of a and streamwise-cross-sectional area of the RBC obtained under the conditions of larger DI indicating larger deformation of RBC.

The relation between DI and the integrated area of ΔR , A_{peak} , is plotted in Fig. 3. A_{peak} increases linearly with an increase in DI . These results indicate the validity of evaluating the deformability of a single RBC by measuring the pattern of ΔR .

Further discussions on the effects of other parameters, such as H_2 , h , and w_s will be shown in the poster.

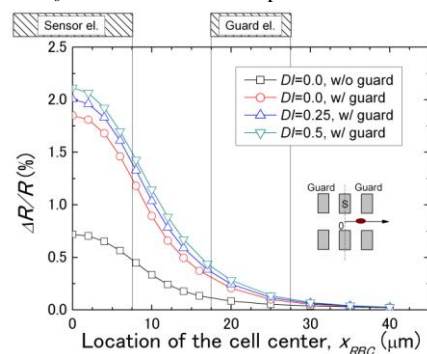


Fig. 2 Relation between the resistance and the cell streamwise displacement from the center of sensor electrodes.

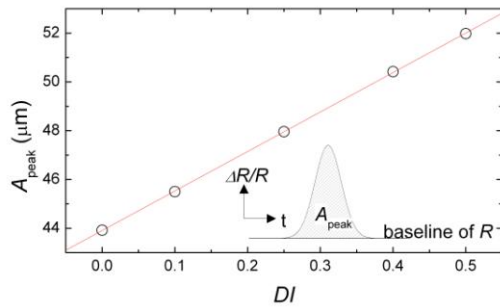


Fig.3 Correlation between the area of $\Delta R/R$, A_{peak} , and DI .

3. EXPERIMENT

Figure 4 shows the schematic view of the channel used in the experiment. The geometrical conditions of channel are specified in Table 1, whose dimensions are same as employed in the numerical simulation. A forward step and side-flows were installed in the channel to control the position of RBC to closely pass the sensing area. RBC from human blood was suspended in the solvent (phosphate-buffered saline with poly-vinylpyrrolidone), and then this RBC solution was supplied to the central channel, while only solvent to the side-flows.

Figure 5 shows the temporal profiles of R obtained by the electric sensors in the preliminary experiments. Each major peak in the distributions indicates the period when an individual RBC crosses the sensor. A_{peak} was estimated using ΔR , the difference from the baseline of the signals for each RBC. The images of RBCs are measured simultaneously by a high-speed camera, and the DI of individual RBCs are obtained from these results. The correlation function between A_{peak} and DI is then calculated and applied to the final validation experiment. More details on the present method will be discussed in the poster.

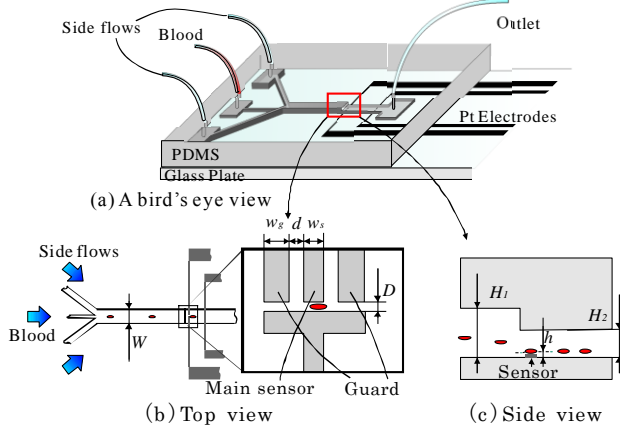


Fig.4 Schematic view of the micro-channel and Pt electrodes.

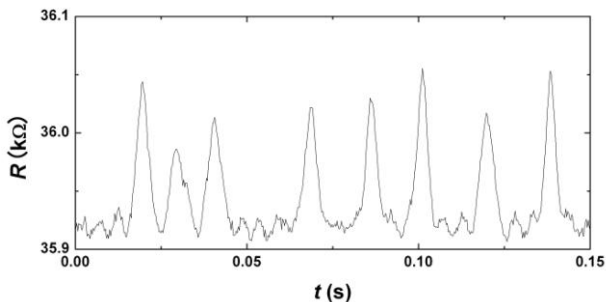


Fig.5 Time series of the resistance between the electrodes.

Table 1 Parameters employed in the simulation & experiment.

Parameter	Dimensions
Channel width, W	1000 μm
Channel height, H_1	50 μm
Channel height at the sensor, H_2	15 μm
Height of the RBC's center, h	5 μm
Volume of deformed RBC, V	$\frac{4}{3}3^3\pi\mu\text{m}^3$
Distance between the electrodes, D	10 μm
Dist. between the sensor and guard, d	10 μm
Width of the sensor electrodes, w_s	15 μm
Width of the guard electrodes, w_g	10 μm

REFERENCES

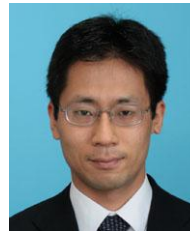
- Korin, N., Bransky, A., and Dinnar, U., Theoretical model and experimental study of red blood cell deformation in microchannels, *J. Biomech.*, vol. 40, no. 9, pp. 2088 – 2095, 2007.
- Tang, H. and Gao, Y., An impedance microsensor with coplanar electrodes and vertical sensing apertures, *IEEE Sensors J.*, vol. 5, no. 6, pp. 1346 – 1352, 2005.
- Gawad, S., Cheung, K., Seger, U., Betsch, A., and Renaud, P., Dielectric spectroscopy in a micromachined flow cytometer: theoretical and practical considerations, *Lab Chip*, vol. 4, pp. 241 – 251, 2004.



Y. Katsumoto received M.E. (2001) in Kyoto Univ. Dept. Mech. Eng. He is now a PhD course student of Dept. of Mech. Engineering and Science, Kyoto Univ. His interests include nondestructive sensing of biological cells and biopolymer, and thermo-fluid dynamics involved in them.



T. Doi received the B.E. (2007) in Kyoto Univ. and is now in the 2nd-year of Master course of Dept. of Mechanical Engineering and Science, Kyoto Univ. His current interests include measurements of fluid flow and blood cells in micro channels.



K. Tatsumi received M.E. (1999) and PhD (2003) in Kyoto Univ. Dept. Mech. Eng. He is now an Assistant Professor of Dept. of Mech. Eng. and Science, Kyoto Univ. His current interests include measurements and simulations of micro biological flows, multi-jets and compact heat exchangers.



K. Nakabe received M.E. (1983) in Kyoto Univ. Dept. Mech. Eng. and PhD (1991) in Osaka Univ. Dept. Mech. Eng. He is now a Prof. of Dept. Mech. Eng. & Science, Kyoto Univ. His current interests are in the fields of turbulent mixing, micro fluidics, heat transfer and combustion.